Acta Oceanol. Sin., 2020, Vol. 39, No. 3, P. 130–140
https://doi.org/10.1007/s13131-020-1564-6
http://www.hyxb.org.cn
E-mail: hyxbe@263.net

Real-time quality control of data from Sea-Wing underwater glider installed with Glider Payload CTD sensor

Zenghong Liu[1, 2*], Jianping Xu[1, 2], Jiancheng Yu[3]

[1] State Key Laboratory of Satellite Ocean Environment Dynamics, Second Institute of Oceanography, Ministry of Natural Resources, Hangzhou 310012, China

[2] Second Institute of Oceanography, Ministry of Natural Resources, Hangzhou 310012, China

[3] State Key Laboratory of Robotics, Shenyang Institute of Automation, Chinese Academy of Sciences, Shenyang 110016, China

Received 28 February 2019; accepted 3 June 2019

Abstract

Profiles observed by Sea-Wing underwater gliders are widely applied in scientific research. However, the quality control (QC) of these data has received little attention. The mismatch between the temperature probe and conductivity cell response times generates erroneous salinities, especially across a strong thermocline. A sensor drift may occur owing to biofouling and biocide leakage into the conductivity cell when a glider has operated for several months. It is therefore critical to design a mature real-time QC procedure and develop a toolbox for the QC of Sea-Wing glider data. On the basis of temperature and salinity profiles observed by several Sea-Wing gliders each installed with a Sea-Bird Glider Payload CTD sensor, a real-time QC method including a thermal lag correction, Argo-equivalent real-time QC tests, and a simple post-processing procedure is proposed. The method can also be adopted for Petrel gliders.

Key words: Sea-Wing underwater glider, Glider Payload CTD sensor, thermal lag correction, quality-control tests

Citation: Liu Zenghong, Xu Jianping, Yu Jiancheng. 2020. Real-time quality control of data from Sea-Wing underwater glider installed with Glider Payload CTD sensor. Acta Oceanologica Sinica, 39(3): 130–140, doi: 10.1007/s13131-020-1564-6

1 Introduction

Underwater gliders are underwater autonomous vehicles first conceived and developed by Henry Stommel and Doug Webb in 1989 (Stommel, 1989). Gliders are able to follow a sawtooth pattern through a combination of vertical and horizontal movements based on a buoyance control system, adjustments in attitude, and adjustments of small fins (Rudnick et al., 2004; Garau et al., 2011). Glider vehicles are designed to autonomously dive to a water depth of typically up to 1 000 m and return to the sea surface along a predetermined path. During their diving and climbing stages, the vehicles observe the water column with various sensors equipped. Therefore, a specific glider mission often consists of several diving and climbing profiles (or downcasts and upcasts). Gliders currently serve as an important tool for oceanographic monitoring from coastal waters to open oceans owing to their capacity to operate autonomously in all weather conditions on missions lasting up to several months. Several commercial products, such as the Slocum glider manufactured by Teledyne Webb Research Corporation, Seaglider developed by the Applied Physics Laboratory at the University of Washington and now available through Kongsberg Maritime, and the Spray glider of the Scripps Institution of Oceanography and Bluefin Robotics, are now widely used in integrated ocean observing systems (e.g., United States Integrated Ocean Observing System (IOOS), Ocean Networks Canada, and the European Gliding Observatories Network), eddy monitoring from the sub-mesoscale to mesoscale (Ruiz et al., 2009; Bouffard et al., 2010, 2012; Baird et al., 2011), upper ocean monitoring from the hurricane pathway (Baltes et al., 2014; Miles et al., 2015), and providing high-resolution in-situ data to data assimilation and model forecasts (Shulman et al., 2009; Dobricic et al., 2010; Pan et al., 2011, 2014; Gangopadhyay et al., 2013; Dong et al., 2017).

In China, the development of the underwater glider began in 2003 and the first prototype named Sea-Wing was developed by the Shenyang Institute of Automation, Chinese Academy of Sciences (CAS) in 2005 (Yu et al., 2011). Another product is the Petrel underwater glider, developed by Tianjin University in 2009 (Liu et al., 2017). These two types of glider were adopted to monitor and understand the dynamics and structure of mesoscale eddies (Shu et al., 2016, 2018; Liu et al., 2019). Like the Slocum glider, both Sea-Wing and Petrel gliders have installed a Sea-Bird Glider Payload conductivity–temperature–depth (CTD) sensor (GPCTD hereafter), with a continuous sampling frequency of ~1 Hz.

Temperature and salinity are the most commonly used variables in oceanography. Temperature is observed directly with a specific sensor while salinity is calculated from measurements of conductivity and temperature using state equations (UNESCO, 1981). Like conventional CTD sensors, there is a misalignment in GPCTD sensor mounted on Sea-Wing gliders because the temperature and conductivity sensors are located downstream of one

Foundation item: The National Natural Science Foundation under contract Nos 41621064, 41606003, U1709202 and U1811464; the National Key R&D Program of China under contract No. 2016YFC0301201; the China Association of Marine Affairs ("Study on the feasibility of establishing an international data sharing application platform for smart ocean").
*Corresponding author, E-mail: liuzenghong@139.com

another, while the thermal inertia of the conductivity sensor introduces a cell thermal mass error in conductivity values and subsequently their derived parameters, such as water salinity and density. In other words, the conductivity cell has mass and the capacity to store heat and it therefore takes time for the conductivity sensor to adjust to the surrounding water, whereas the temperature sensor has a more rapid response time. Because conductivity is a strong function of temperature, a small change in water temperature inside the conductivity cell causes largely erroneous salinity values, especially across the thermocline. It is therefore important to conduct a thermal lag correction for both the downcast and upcast before using observations in scientific research. A practical method of correcting for heating inside the cell was developed by Morison et al. (1994). Garau et al. (2011) proposed a new method of correcting the thermal lag error associated with unpumped CTD sensors deployed on Slocum gliders. Liu et al. (2015) recently suggested practical procedures of correcting the thermal lag of salinity data recorded by an unpumped CTD sensor across a sharp thermocline.

Besides the thermal lag correction, a robust quality control (QC) procedure for temperature and salinity data obtained from gliders is also critical. The IOOS program drafted a real-time QC manual for CTD data obtained from gliders (U.S. Integrated Ocean Observing System, 2016), where a total of 19 tests are implemented. Tintoré et al. (2013) and Troupin et al. (2015) developed a Matlab-based glider toolbox (named the SOCIB Glider toolbox, https://github.com/socib/glider_toolbox) for processing glider data, correcting the thermal lag of salinity, and displaying data. However, like the CTD sensor mounted on Argo profiling floats, the CTD sensor, especially the conductivity sensor used on underwater gliders, may experience sensor drift owing to biofouling, biocide leakage into the conductivity cell, and a variety of other problems several months after their deployment (Wong et al., 2003; Oka and Ando, 2004; Liu et al., 2007). A comparison between the glider temperature and salinity profiles and a high-quality historical hydrographic data set or WOA climatology is thus necessary because profiles for which there has been sensor drift usually have good shapes and cannot be detected in real-time QC tests.

As technical development of the underwater glider progresses and the application of the underwater glider in oceanographic research and operational forecasts in China grows, the QC of data from either Sea-wing or Petrel gliders becomes increasingly important. On the basis of temperature and salinity profiles obtained by Sea-Wing underwater gliders, the present paper proposes a complete processing method that involves a thermal lag correction, real-time QC procedure involving 12 QC tests, and post-processing approach.

2 Main features of Sea-Wing gliders

Three types of Sea-Wing underwater glider have been developed by the Shenyang Institute of Automation, CAS, namely 1 000-, 4 500-, and 7 000-m models. The present paper uses only the 1 000-m model because it has been more widely adopted than the other models in field investigations. The Sea-Wing glider has a mass of ~65 kg, a length of ~2 m, and the capacity to carry an additional ~3 kg of sensors. The glider is powered by batteries and can be deployed for up to 5 months, allowing 3 000 km of transections of water column (0–1 000 m) data to be sampled. The forward speed of the glider is approximately 0.3 m/s and varies depending on the predetermined path, mission duration, water density, and ocean front. The glider's ascent/descent (Fig. 1) speeds vary through the water column depending on the glider's

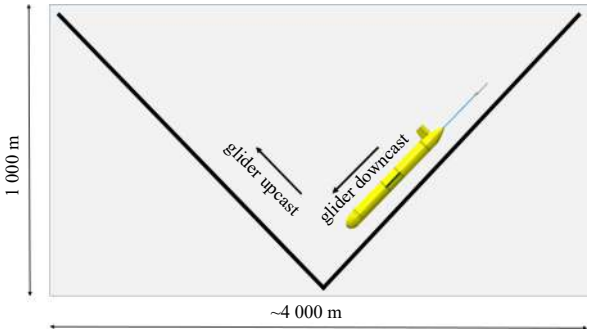

Fig. 1. Schematic view of the Sea-Wing underwater glider sampling design.

buoyancy adjustment and attitude and the water density. With pressure and time data recorded on eight investigation cruises and by eight gliders between 2014 and 2016 in the South China Sea (SCS), the average descent/ascent speeds versus water pressure are estimated and shown in Fig. 2. It is clear that the descent speed is much more variable than the ascent speed, with the descent speed reaching a maximum value of 0.67 m/s around a depth of 50×10^4 Pa. The descent speed decreases rapidly between 50×10^4 and 200×10^4 Pa, where the pycnocline is located, and after that gliders maintain a mean descent speed of about 0.16 m/s until they reach their maximum profiling depth (~1 000 m). Meanwhile, the ascent speed is fairly stable, with an average value of about 0.23 m/s. A Sea-Wing glider takes approximately 1.85 h on average to dive from the sea surface to a depth of 1 000 m and 1.49 h to climb from a depth of 1 000 m to the sea surface.

Each Sea-Wing glider is installed with a Sea-Bird GPCTD sensor. Considering the data transmission rate, Sea-Wing gliders are currently programmed to record a CTD sample for a 6-s interval. When a CTD sample is required, the GPCTD pump turns on and produces a constant flow rate of ~0.01 L/s; i.e., the speed of the flow through the temperature sensor and conductivity cell is fixed and known, which makes the thermal lag correction more effective than that for unpumped CTDs (e.g., SBE41 CTD), where the flow rate varies depending on the angle and speed of the glider (Liu et al., 2015).

3 Processing of glider CTD data

3.1 *Time conversion*

Pressure, temperature, and conductivity measurements and associated time information are reported by Sea-Wing gliders. In addition, a Global Positioning System (GPS) fix and time stamp is obtained when the glider starts to dive or reaches the sea surface from underwater. A precise duration calculation often applies the UNIX epoch, which is the number of seconds that have elapsed since 1 January 1970 (midnight UTC/GMT). Therefore, all the date and time information for both CTD measurements and GPS fixes are converted into the UNIX epoch time before processing.

3.2 *Conductivity anomaly detecting*

Because sea water salinity is computed from the conductivity, temperature, and pressure measured by a GPCTD sensor on the Sea-Wing glider, it is necessary to detect and exclude abnormal conductivity induced by the behavior of the glider or biofouling on the CTD sensor. When a glider starts to dive or ends its ascending profile, the CTD sensor mounted may be exposed to the air and record abnormal conductivity data. Three QC tests are

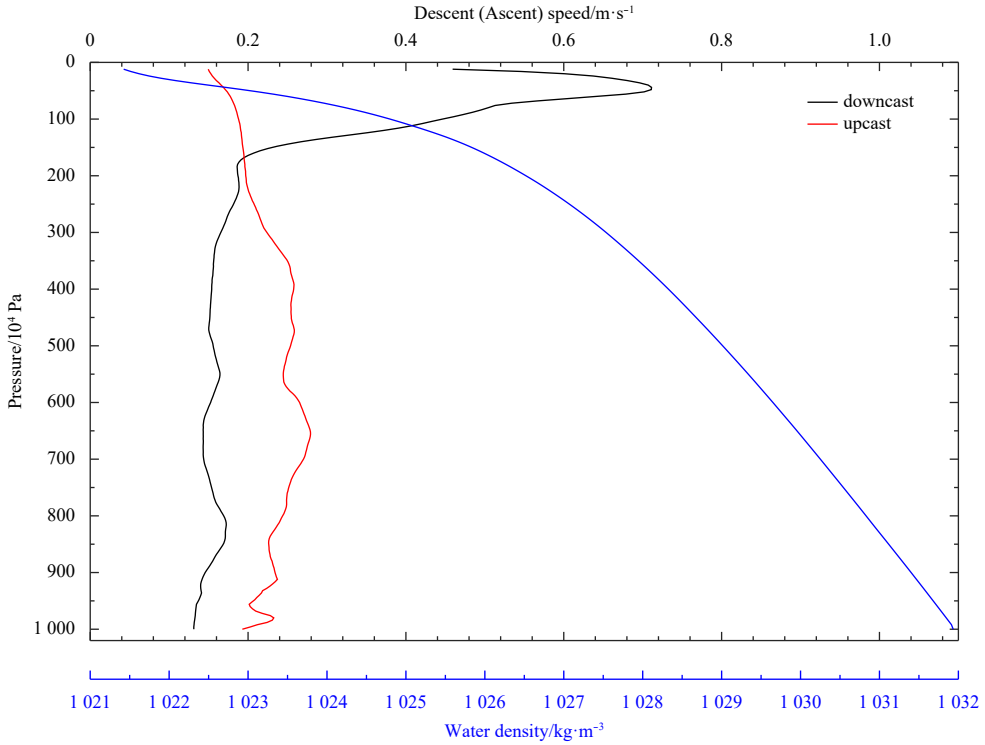

Fig. 2. Average descent (black) and ascent (red) rates of Sea-Wing gliders vs pressure in the northern South China Sea (SCS). The water density is denoted by the blue curve.

conducted to detect erroneous conductivity measurements.

(1) Global range test

The global range test is conducted to detect erroneous conductivity values out of the range of the measurement range of the conductivity sensor; i.e., 0–6 S/m. If any conductivity value fails this test, the conductivity value and its corresponding temperature value are flagged as bad data ("4") and excluded from the further calculation of salinity.

(2) Spike test

Prior to the spike test, the descent and ascent phases of a glider cycle are split into a downcast and upcast. The spike test does not consider differences in pressure but assumes a sampling that adequately reproduces changes in conductivity with pressure. The conductivity value $C(i)$ is flagged as bad if not previously flagged and

$$|C(i)-(C(i+1)+C(i-1))/2|- |(C(i+1)-C(i-1))/2|>K, \quad (1)$$

where C is the conductivity and i is the start-to-end array index of the profile, $K=0.15$ S/m ($Z(i)<500\times10^4$ Pa) or $K=0.02$ S/m ($Z(i)\geqslant 500\times10^4$ Pa), and Z is the pressure.

(3) Running standard-deviation test

The running standard-deviation algorithm is taken from the United States IOOS Glider DAC QC manual. The values of the running average ($Cave(i)$) and standard deviation ($Cstd(i)$) over nine consecutive points (if not previously flagged as bad) are computed for each $i=4$ to $N-3$ (where N is the total number of points in a profile). The preceding and succeeding points are not used in the calculation if the time interval between adjacent points is greater than 30 s or the depth interval is greater than 5×10^4 Pa. For the first (last) four points of the time series, the average and standard deviation are computed as for the fifth (N–4th) value.

A conductivity value should be flagged as bad if not previously flagged and both $|C(i)-Cave(k)|>2.2\times Cstd(i)$ and $|C(i)-Cave(k)|>0.001$ S/m (the assumed approximate minimum resolution of the GPCTD conductivity measurement).

3.3 *Thermal lag correction*

A thermal lag correction should be applied prior to the QC of the glider observations. A Matlab script from the SOCIB Glider toolbox is employed for the thermal lag correction of Sea-Wing gliders installed with a GPCTD sensor. This script adopts the approach developed by Lueck and Picklo (1990). They expressed the conductivity correction (C_T) as

$$C_T(n)=-bC_T(n-1)+\gamma a[T(n)-T(n-1)], \quad (2)$$

where n is the sample index, T is the temperature, and γ is the sensitivity of conductivity to temperature given by the manufacturer. The coefficients a and b are given as

$$a=\frac{4f_n\alpha\tau}{1+4f_n\tau}, \quad (3)$$

$$b=\frac{1-2a}{\alpha}, \quad (4)$$

where f_n is the Nyquist sampling frequency and α and τ are respectively the amplitude of the error and time constant. Both α and τ depend on the flow speed through the conductivity cell. On the basis of conventional CTD methodology, in which the flow speed is constant because it is controlled manually in a CTD op-

eration, Morison et al. (1994) suggested α and τ be expressed as

$$\alpha = 0.013\ 5 + 0.026\ 4/V, \tag{5}$$

$$\tau = 7.149\ 9 + 2.785\ 8/\sqrt{V}, \tag{6}$$

where V is the average velocity (having units of m/s) through the conductivity cell. Considering the variable speed of the glider, Garau et al. (2011) gave the above two equations as

$$\alpha(n) = \alpha_o + a_s/V(n), \tag{7}$$

$$\tau(n) = \tau_o + \tau_s/\sqrt{V(n)}, \tag{8}$$

where the subscripts o and s respectively indicate the offsets and slopes. The determination of the parameters α_o, a_s, τ_o, and τ_s is critical in the thermal lag correction. On the basis of the hypothesis that the downcast and upcast CTD profiles measure the same water mass (assuming a low horizontal advection), Garau et al. (2011) proposed a practical method of determining those parameters by minimizing an objective function that measures the area between two T–S curves from the sequent downcast and upcast of a glider. After correction of the thermal lag, salinity is calculated from conductivity, temperature, and pressure measurements using state equations (UNESCO, 1981).

Conductivity is a strong function of temperature as mentioned above, and an increasing mismatch between the temperature in the conductivity cell and ambient water therefore leads to a remarkable salinity error. To illustrate the thermal lag effect in different water columns, we selected three profiles (downcast and upcast) recorded by GPCTD sensors on two Sea-Wing gliders (Fig. 3). The downcast and upcast of each profile were observed within 3 km spatially and 4 h temporally. Figures 3a–c presents observations obtained by Glider 1000J003 operating in the SCS on 5 July 2016 under conditions of a relatively weak thermocline (the average temperature gradient was 0.09°C/m between 20×10^4 and 80×10^4 Pa) and shallow mixed layer depth (MLD) of ~20×10^4 Pa. No thermal lag effect is evident, and the salinity difference between the downcast and upcast is only ~0.05 between 60×10^4 and 180×10^4 Pa. Figures 3d–f presents observations obtained by the same glider except that the profile was observed in the northern SCS on 8 May 2015. In this case, the thermocline is stronger with an average temperature gradient of about 0.13°C/m in the range of 20×10^4–80×10^4 Pa. A salinity difference between the downcast and upcast is evident above a depth of 200×10^4 Pa, with the difference being a maximum of ~0.35 around a depth of 50×10^4 Pa (Fig. 3e). The salinities from the downcast are higher than those from the upcast between 30×10^4 and 200×10^4 Pa. This appreciable salinity difference is obviously induced by the thermal lag effect and larger temperature gradients when the glider crosses the thermocline. Using the Matlab script from the SOCIB Glider toolbox, the thermal lag was corrected with an initial guess for α and τ of 0.067 7 and 11.143 1, respectively. Here, an estimated constant flow rate of ~0.486 7 m/s (V) from reported Sea-Bird GPCTD specifications is applied. The correction effect is evident for the downcast around depths of 40×10^4 to 160×10^4 Pa in the water column, where the salinities are corrected by as much as about –0.3 (Fig. 3e), which is equivalent to the result reported by Garau et al. (2011). In the case of a relatively weak thermocline (Fig. 3a), the thermal lag correction for the downcast is much smaller than that in the case of the strong thermocline, with the maximum correction being only about –0.05 at a depth of 70×10^4 Pa. The last case is that of Glider 1000K003 located east of the Luzon Strait (near 19.28°N and 122.58°E) on 10 October 2016 (Figs 3g–i). The temperature gradient is only 0.04°C/m between 20×10^4 and 80×10^4 Pa while the MLD is thick (~80×10^4 Pa). The thermal lag effect is almost negligible, such that the downcast and upcast salinities coincide well. The thermal lag correction across a weak thermocline is also negligible in this case.

Statistically, below the mixed layer, the downcast salinities after thermal lag correction are lower than the raw salinities directly computed from the reported conductivities (Fig. 4). In particular, the amplitude of the correction can be larger than 0.1 at water depths of 50×10^4 –60×10^4 Pa with strong temperature gradients. In contrast, the upcast salinities after thermal lag correction are generally higher than the raw salinities throughout the water column, but the amplitude of the correction across a strong temperature gradient is much smaller than that for the downcast. The reason why the thermal lag effect is more remarkable for the downcast is not clear and requires further investigation.

3.4 *Procedures for glider real-time QC tests*

Because the underwater glider has a mission schematic and CTD sensor similar to those of the Argo profiling float, the real-time QC tests being applied to Argo can also be adopted for gliders; e.g., the United States IOOS Glider data assembly center (DAC) has developed QC tests referring to Argo (U.S. Integrated Ocean Observing System, 2016). In the real-time QC of Argo CTD data, about 16 tests are automatically conducted by computers, including tests for the profile location, date and time, drifting speed, density inversion, stuck values, global/regional range, deepest pressure, spikes, and gradients of temperature and salinity profiles (Wong et al., 2019). It is worth noting that a climatological test strongly recommended by the glider community has not yet been adopted in Argo real-time QC, probably because delayed-mode QC methods (Wong et al., 2003; Böhme and Send, 2005; Owens and Wong, 2009) have been adopted to calibrate Argo salinity profiles using a global high quality and high-resolution hydrographic data set. However, in our work, when we develop a real-time QC tool for Sea-Wing gliders, a climatological test is considered together with Argo-equivalent QC tests.

(1) Date test

The date test requires that the Julian day (JULD) of a glider downcast/upcast profile be later than 1 January 2010 and earlier than the current date of the check (in UTC time). If JULD denotes the number of days that have elapsed since 1 January 1970, then the date of a glider profile fails the test when JULD < 14 610 or JULD > UTC date of the test. The date of the profile is flagged as bad data ("4") and none of the data from the profile are used.

(2) Position test

First, the observation latitude and longitude of a glider profile should be between –90° and 90° and between –180° and 180° respectively. If either the latitude or longitude fails this test, the profile position is flagged as bad data and none of the data from the profile are used.

Second, the profile position should be located in an ocean. We make use of the global 5-min bathymetry data set (ETOPO5/TerrainBase), which can be downloaded from http://iridl.ldeo.columbia.edu/SOURCES/.NOAA/.NGDC/.ETOPO5/datasetdatafiles.html. If a position cannot be located in an ocean, the profile is flagged as bad data.

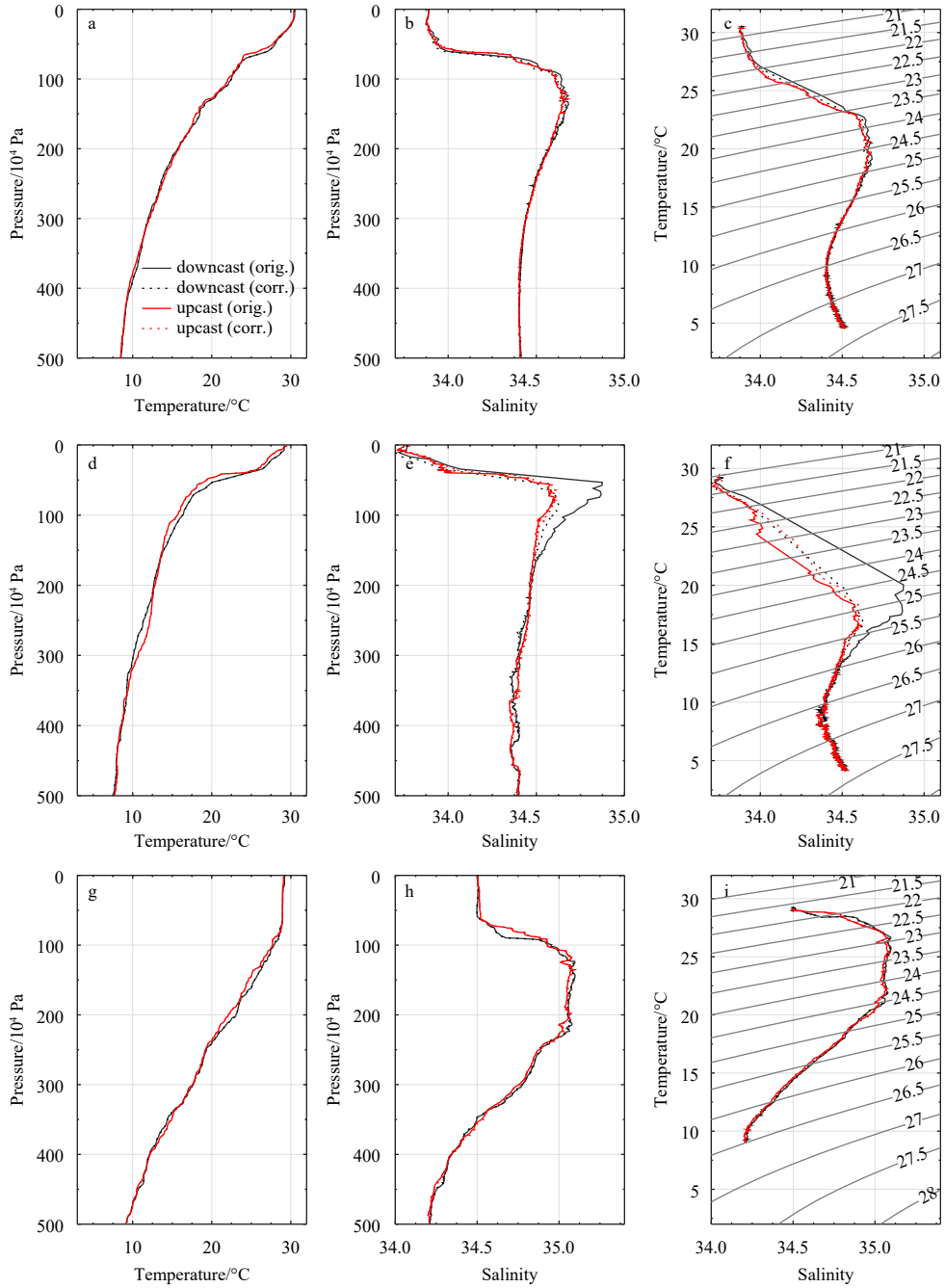

Fig. 3. Temperature, salinity profiles and temperature–salinity curves from Sea-Wing gliders' downcast (black) and upcast (red). a–c. Observed in the SCS (around 17.04°N, 113.44°E) by Sea-Wing glider 1000J003 on 5 July 2016; d–f. from Sea-Wing glider 1000J003, but observed at about 20.21°N, 118.30°E on 8 May 2015; and g–h. Sea-Wing glider 1000K003 east of the Luzon Strait (~ 19.28°N, 122.58°E) on 10 October 2016. The original and corrected downcast results are respectively shown as solid and dotted black lines whereas the upcast results are shown as red lines.

(3) Pressure test

All pressure measurements in seawater should be larger than 0 Pa. If any pressure fails this test, the pressure and its corresponding temperature and salinity are flagged as bad data. In addition, if we know the preprogrammed maximum profiling depth (DEEPEST_PRES) of an underwater glider, a deepest-pressure test can be conducted as no pressure measurement of a profile should be greater than 1.1 × DEEPEST_PRES.

(4) Global range test

A gross filter is applied to observations of temperature and salinity. The ranges need to accommodate all expected extremes that may occur in the oceans; i.e., temperatures in the range of −2.5 to 40.0°C and salinity in the range of 0 to 41.

(5) Stuck profile test

The stuck profile test looks for measurements of temperature and salinity in a profile being identical. Each point in a profile is flagged as bad if the difference between the minimum and maximum values on the profile is less than the resolution of the CTD sensor; i.e., $\max(T(i)) - \min(T(i)) < 0.001$°C and $\max(S(i)) - \min(S(i)) < 0.001$, where T and S are respectively the temperature

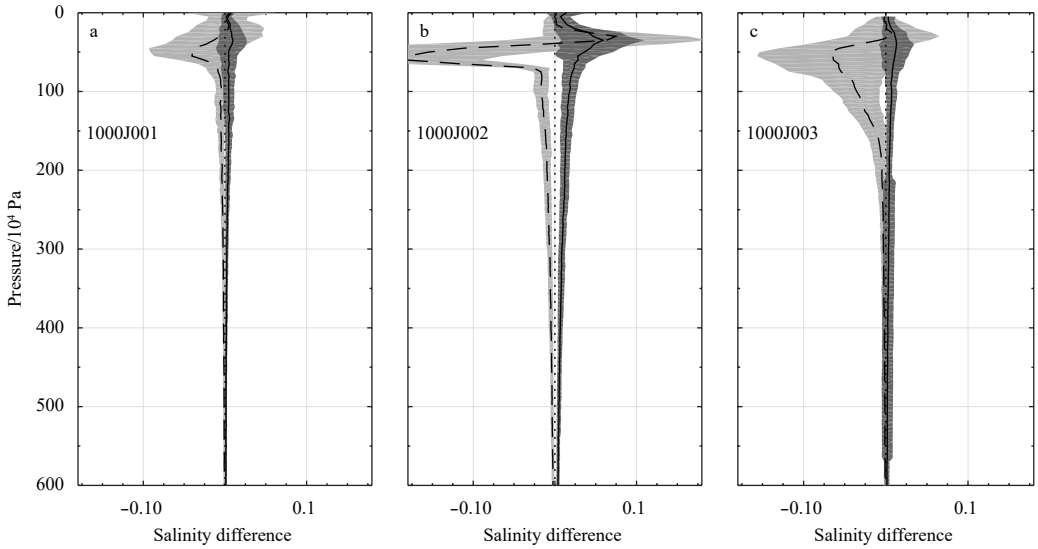

Fig. 4. Mean difference between thermal-lag-corrected and raw salinities for downcast (dashed lines) and upcast (black solid lines) from Glider 1000J001 (a), 1000J002 (b) and 1000J003 (c) . The standard deviation of the salinity difference is denoted by gray shading.

and salinity, and i is the start-to-end array index of the profile.

(6) Spike test

The spike test uses the same algorithm as that used for conductivity; i.e., Eq. (1).

For temperature ($T(i)$):

temp_flag(i) = 4 if not previously flagged and

$$|T(i) - (T(i+1) + T(i-1))/2| - |(T(i+1) - T(i-1))/2| > K, \quad (9)$$

where K = 6°C ($Z(i)$ < 500×10⁴ Pa) or K = 2°C ($Z(i) \geqslant$ 500×10⁴ Pa) and Z is the pressure.

For salinity ($S(i)$):

salt_flag(i) = 4 if not previously flagged and

$$|S(i) - (S(i+1) + S(i-1))/2| - |(S(i+1) - S(i-1))/2| > K, \quad (10)$$

where K = 1.0 ($Z(i)$ < 500×10⁴ Pa) or K = 0.5 ($Z(i) \geqslant$ 500×10⁴ Pa).

(7) Gradient test

The gradient test is failed when the difference between vertically adjacent measurements is too great. The test does not consider differences in pressure but assumes a sampling that adequately reproduces changes in temperature and salinity with pressure. The algorithm from the United States IOOS Glider DAC QC manual (U.S. Integrated Ocean Observing System, 2016) is adopted here.

For temperature:

temp_flag(i) = 4 and temp_flag(i+1) = 4 if not previously flagged and

$$|(T(i+1) - T(i))/(Z(i+1) - Z(i))| > K, \quad (11)$$

where K = 2°C/10⁴ Pa ($Z(i$+1) $\leqslant$ 5×10⁴ Pa), K = 8°C/10⁴ Pa (5×10⁴ Pa < $Z(i$+1) $\leqslant$ 500×10⁴ Pa), K = 2°C/10⁴ Pa ($Z(i$+1) > 500×10⁴ Pa).

For salinity:

salt_flag(i) = 4 and salt_flag(i+1) = 4 if not previously flagged and

$$|(S(i+1) - S(i))/(Z(i+1) - Z(i))| > K, \quad (12)$$

where K = 0.3/10⁴ Pa ($Z(i$+1) $\leqslant$ 5×10⁴ Pa), K = 1.7/×10⁴ Pa (5×10⁴ Pa < $Z(i$+1) $\leqslant$ 500×10⁴ Pa), K = 0.15/10⁴ Pa ($Z(i$+1) > 500×10⁴ Pa).

(8) Running standard-deviation test

The running standard-deviation test employs the same algorithm as that used for conductivity in Section 3.2.

For temperature:

temp_flag(i) = 4 if not previously flagged and both $|T(i) - Tave(k)| > 2.2 \times Tstd(i)$ and $|T(i) - Tave(k)| > 0.001$ (temperature resolution of the GPCTD).

For salinity:

salt_flag(i) = 4 if not previously flagged and both $|S(i) - Save(k)| > 2.2 \times Sstd(i)$ and $|S(i) - Save(k)| > 0.001$ (salinity resolution of the GPCTD).

(9) Racape's spike test

A new spike test is based on the method presented by Racape et al. (2018) at the 19th meeting of the Argo data management team (San Diego, U.S.A., December 2018) and is expected to be applied to Argo real-time QC in the future. In the method, a five-point moving median is suggested and computed along the entire profile (while the median value is computed if there are fewer than five points). If the difference between the observed value and its associated moving median is greater than a given standard deviation, the value is flagged as bad data ("4"). The thresholds of the temperature and salinity standard deviations depend on depth and have spatiotemporal variability. One can compute a global-ocean monthly temperature and salinity standard deviation climatology using the WOA or other datasets. We here use thresholds similar to those given by Racape et al. (2018) as shown in Table 1. Figure 5 shows an example of the test for a given salinity profile. Two successive salinity anomalies around a depth of 500×10⁴ Pa and three at depths between 700×10⁴ and 800×10⁴ Pa are defined manually prior to testing. Results show that Racape's spike test screened the former two successive anomalies successfully but failed to screen the latter three success-

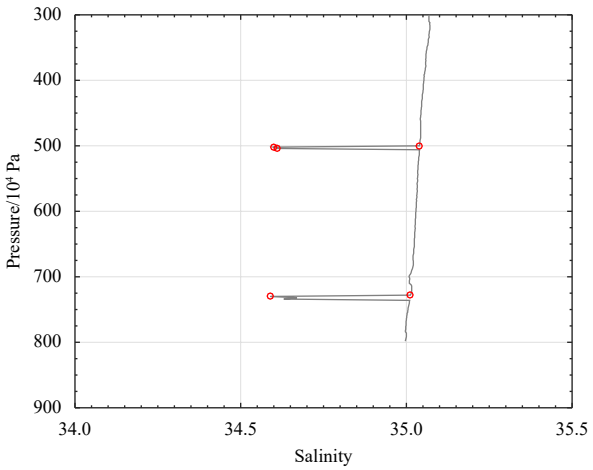

Fig. 5. Vertical salinity profile for Racape's spike test. Open red circles indicate the salinities that failed Racape's spike test.

ive anomalies. The new spike test is thus limited and can detect no more than two successive spikes efficiently.

(10) Density inversion test

Before the density inversion test, the potential density is computed using the Matlab seawater toolbox (http://www.cmar.csiro.au/datacentre/ext_docs/seawater.htm). From top to bottom, if the potential density calculated at the greater pressure $Z(i+1)$ is less than that calculated at the lesser pressure $Z(i)$ by more than 0.03 kg/m^3, both the temperature and salinity values at $Z(i)$ and $Z(i+1)$ are flagged as bad data.

(11) Vertical velocity test

Figure 2 shows that the vertical speed of a Sea-Wing glider is no lower than 0.1 m/s on average. We define 0.03 m/s as the threshold of vertical velocity, and any pressure, temperature, and salinity measurements excluding data shallower than 10×10^4 Pa and 10×10^4 Pa shallower than the maximum profiling depth should be flagged as bad data if the calculated vertical velocity is less than 0.03 m/s. This test ensures that observations made by a Sea-Wing glider are obtained during a period of good behavior and pitch change of the glider.

(12) Climatological test

A climatological test is strongly recommended for the real-time QC of gliders because a sensor on a glider may drift several months after the glider's deployment. This sensor drift usually results in a systematic error in the temperature or salinity profile that is difficult to detect in Argo-equivalent QC tests. A good climatology data set can be used to visually inspect the quality of temperature and salinity profiles and detect potential sensor drift. We here choose the historical hydrographic data set maintained by the Coriolis data center (IFREMER) as the climatology data set that we will apply in the glider climatological test. Each shipboard CTD profile contained in the data set has been visually checked by the operator at the Coriolis data center. The data set (named the DMQC_Argo CTD dataset) is not publicly available and can only be used in Argo delayed-mode QC. In addition, considering the many gaps, especially in the Southern Ocean (Fig. 6), we downloaded the WOA2018 climatology (Garcia et al., 2019) as an alternative to the DMQC_Argo CTD dataset. However, a global climatology data set usually has many profiles, which reduces the search speed when we conduct a climatological test for profiles one by one. We therefore separated both the DMQC_Argo CTD and WOA18 data sets into many small boxes (10° × 10°), which is expected to accelerate our data search.

The temperature/salinity mean and standard deviation are calculated as functions of the standard depth for the DMQC_Argo CTD data set using all the temperature/salinity profiles in each box, whereas existing standard deviations in the WOA18 are directly used. In the climatological test for our glider, according to the GPS fix of a downcast/upcast profile, a corresponding box is searched for either from the DMQC_Argo CTD or WOA18. Both the temperature and salinity standard-deviation profiles are linearly interpolated to the glider's vertical level. The glider-observed profile and mean climatological profile are then compared. If the difference between the two profiles is larger than

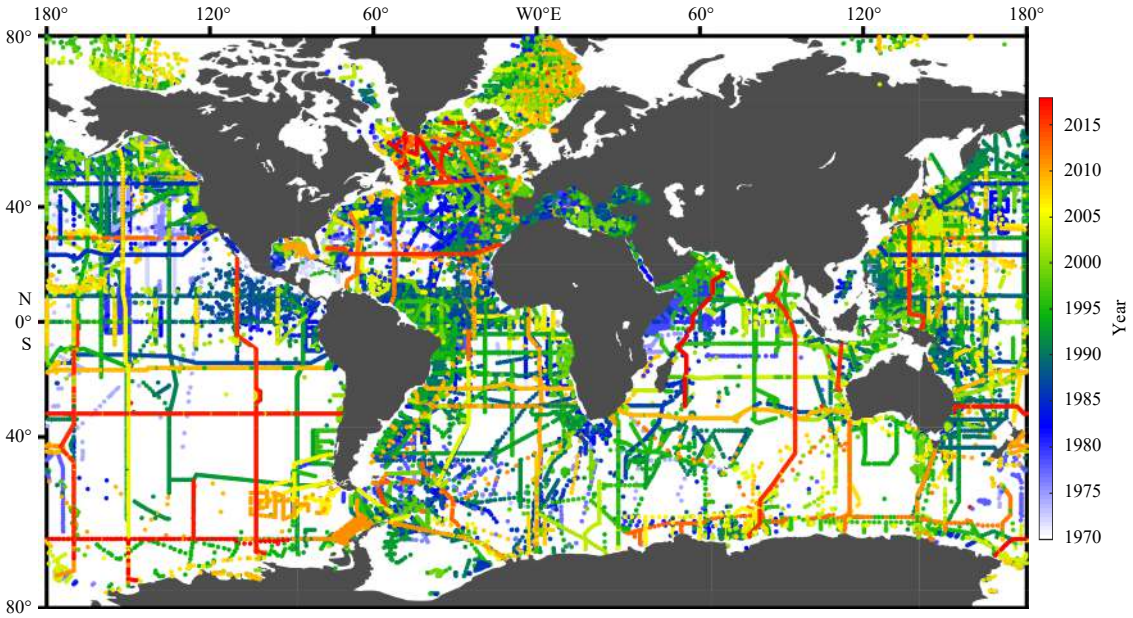

Fig. 6. Scatter plot of the profile positions from the DMQC_Argo CTD dataset. Colors indicate the years in which profiles were observed.

n_std × Qstd(i), then the corresponding value should be flagged as doubtable ('3'), where Qstd(i) is the temperature or salinity standard deviation from the DMQC_Argo_CTD or WOA18 that we have interpolated to the glider's level and n_std is the multiple factor of the standard deviation that gives the threshold. A robust choice of n_std is expected to accommodate seasonal and long-term ocean variability on a basin scale. The selection of n_std should therefore be made cautiously, which requires the local QC operator to know the regional ocean variability. According to the United States Navy's standard monthly ocean temperature and salinity climatology (GDEM), n_std = 5 was previously used for the United States IOOS Glider DAC, but there were too many cases in which this test was failed even though the temperature and salinity were apparently good (U.S. Integrated Ocean Observing System, 2016). In our work, a larger threshold in the range of 6 to 8 is recommended.

Figure 7 presents an example of the climatological test using temperature and salinity profiles obtained from an Argo profiling float (WMO number: 2902581; cycle number: 93). We did not use data from Sea-Wing gliders because we have not found a profile from the existing glider data set that both contains sensor drift and has good shape. It is clearly seen that the salinity profile of the 93th cycle has a systematic offset against the other profiles (Fig. 7a), which is probably due to biofouling or other technical problems. The entire temperature profile falls into the climatological standard-deviation envelop with n_std = 6 (Fig. 7c), while part of the salinity data fails the test between 400×10^4 and 2 000×10^4 Pa, suggesting that the salinity data from this float contain a positive sensor drift or offset.

3.5 *Post-processing of glider CTD data*

After correcting for thermal lag and conducting the 12 proposed real-time QC tests, the data are clearer and more consistent between downcast and upcast profiles than the raw data. However, mismatches between the downcast and upcast profiles, especially across the thermocline, are not completely eliminated (Fig. 8). The corrected temperature data in the downcast profile tend to be lower than those in the upcast profile. Conversely, the corrected salinity data in the downcast profile are higher than those in the upcast profile. A simple average taken between the

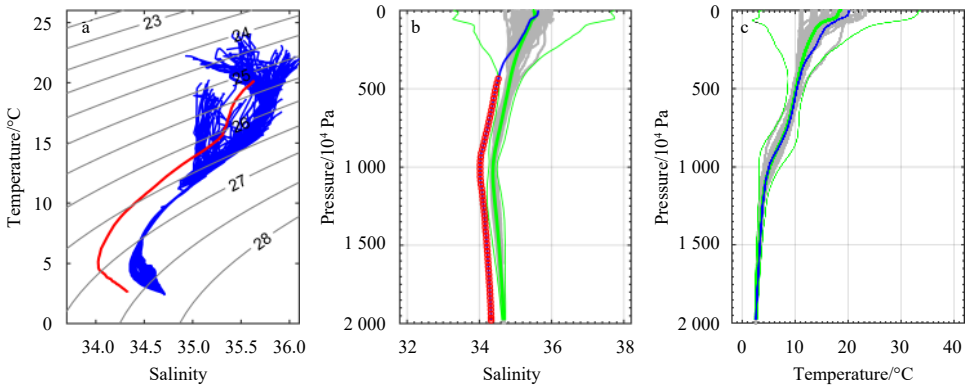

Fig. 7. Example of the glider climatological test. a. Temperature–salinity curves (blue lines) observed by an Argo float (WMO number: 2902581). The abnormal profile (cycle number: 93) is shown in red line. b. The abnormal salinity derived by the Argo float (blue line) and the DMQC_Argo CTD-data-set-derived mean salinity profile (thick green line).The 6 times the standard deviation envelope is denoted by thin green line. c same as b but for temperature. The points that failed the climatological test are marked by red circles. The gray dots are randomly 1/3 profiles in the search box of the DMQC_Argo CTD data set.

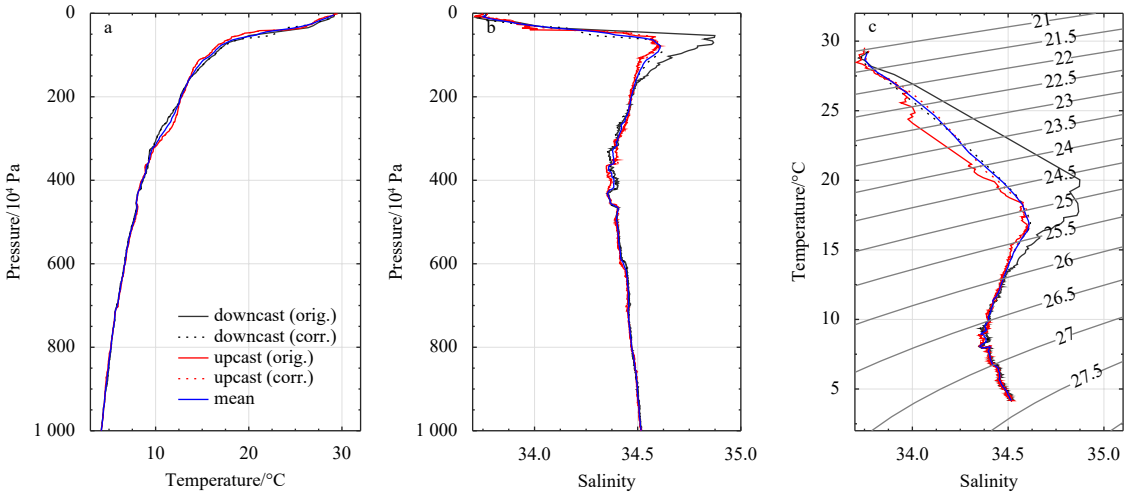

Fig. 8. CTD data observed by Sea-Wing glider 1000J003 in the SCS on May 8, 2015. Temperature (a), salinity profiles (b) and temperature–salinity curves (c) from the glider's downcast (black) and upcast (red). Original and corrected downcast results are respectively shown as solid and dotted black lines whereas the upcast results are shown as red lines. The (five-point) moving mean filtered and average data from the corrected downcast and upcast profiles are shown in blue lines.

downcast and upcast profiles thus seems to be more reasonable if we consider that the two profiles should measure the same water mass. Meanwhile, even large spikes should have been removed by the two spike tests in Section 3.4 and yet small hooks are found in both the temperature and salinity profiles (not shown). To remove these hooks, a moving (five-point) mean filter is strongly suggested before averaging. Afterward, both the corrected downcast and upcast temperature/salinity profiles are first linearly interpolated to the same vertical levels. The two interpolated profiles are then averaged into one single profile. The effect of the moving mean filter and averaging is seen in Fig. 8 (blue lines). In order to illustrate the amplitude of the salinity difference between post-processed and corresponding corrected downcast/upcast profiles, we selected all observations (1 566 profiles in total) from three gliders (1000J001–003) that operated in the SCS. It can be seen from Fig. 9 that the mean salinity differences between post-processed and corrected downcast are almost within ±0.1. The most notable differences are found at depths of 40×10^4–60×10^4 Pa(with the maximum standard deviation being as high as 0.08 for Glider 1000J002), where temperature gradients are strongest. These differences are negligible below 150×10^4 Pa. The upcast profiles have the similar post-processed–corrected salinity differences as the downcast profiles but show an inverse distribution in vertical (not shown)

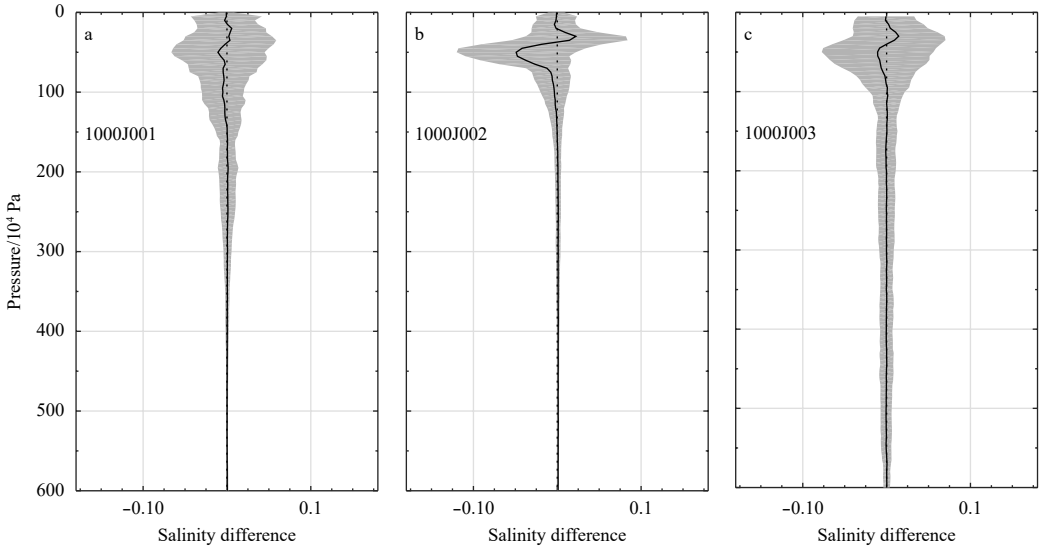

Fig. 9. Mean salinity difference (black solid lines) between post-processed (the averages of the corrected downcast and upcastsalinities after a five-point moving mean filtered) and corresponding corrected downcast profiles for Glider 1000J001 (a), 1000J002 (b) and1000J003 (c). The standard deviation of the salinity difference is denoted by gray shading.

4 Discussion and conclusions

The real-time QC of CTD profiles recorded by underwater gliders usually involves a thermal lag correction, various QC tests (similar to Argo real-time QC tests), and the post-processing of downcast and upcast profiles. Thermal lag effects are generated by the mismatch between the temperature probe and conductivity cell response times. Such a thermal lag effect is more evident when a glider crosses a sharp temperature gradient (strong thermocline). Because the conductivity strongly depends on temperature, the reported thermal-lag-induced salinity error can be up to ~0.3 for a strong thermocline. Without correction of the thermal lag, salinity profiles derived from conductivity observations will contain large errors, especially profiles in areas having a strong thermocline. The correction of the thermal lag effect relies on the flow speed through the conductivity cell. The use of a CTD sensor without a pump system (i.e., an unpumped system) leads to a variable flow speed owing to the variable glider surge speed, which is thought to introduce difficulties to the thermal lag correction. It is therefore strongly recommended that a CTD sensor with a pump system (e.g., a GPCTD or SBE41CP) is installed on a glider. In addition, a high-resolution sampling scheme is required in an area having a sharp thermocline for the better correction of thermal lag. As for a Sea-Wing glider installed with a GPCTD (having a sampling rate of ~1 Hz), we suggest the manufacturer design the glider to record and transmit all original samples instead of subsamples.

It is worth noting that the CTD sensor mounted on a glider can be calibrated in the laboratory either prior to its deployment or after its recovery in contrast to the case of a sensor mounted on an (expendable) autonomous profiling float, which is expected to favor the QC of observations. However, gliders are often deployed in coastal waters, where their sensors are inevitably affected by oil contamination or biofouling. This puts more focus on the QC of their observations than on the QC of the observations of autonomous profiling floats. In particular, the systematic error of each CTD sensor should be known in an observation network comprising tens of co-operating gliders. Besides sensor calibration in the laboratory, *in-situ* comparisons with shipboard CTD casts and analyses conducted using a salinometer are critical. In addition, the establishment of a regional high-quality hydrographic data set is essential to detect sensor drift that may occasionally occur for gliders. We also suggest that the Argo-equivalent target accuracy (i.e., 0.01 for salinity, 0.005℃ for temperature and 2.5×10^4 Pa for pressure) be adopted for gliders in open oceans and some marginal seas, such as the South China Sea.

As the use of CTD data recorded by Sea-Wing gliders increases, an approach for processing these data becomes necessary. It will be meaningful to draft a QC manual and develop a robust toolbox for both the processing and real-time QC of CTD observations made by gliders.

The present paper, on the basis of observations made by Sea-Wing gliders, proposed a complete real-time QC procedure of CTD profiles, involving thermal lag correction, 12 QC tests, and a simple post-processing method. Among the real-time QC tests, a new spike test based on the method proposed by Racape and a climatological test using a high-quality historical hydrographic data set (DMQC_Argo CTD) previously used for Argo delayed-mode QC and WOA climatology were first suggested. The climatological test can be used to detect potential sensor drift given an appropriate threshold (n_std times the standard deviation). It is noted that the behaviors of a glider are also important in determining the glider's vertical velocity and thus the quality of the temperature and salinity profiles. These QC tests could also be adopted for Petrel gliders.

Acknowledgements

This work benefited from numerous freely available data sets and useful toolboxes. The Sea-Wing underwater glider data were provided by the State Key Laboratory of Robotics, Shenyang Institute of Automation, Chinese Academy of Sciences. The WOA2018 climatology was developed by the National Centers for Environmental Information, NOAA and downloaded from https://www.nodc.noaa.gov/OC5/woa18. The DMQC_Argo CTD data set was provided by the Coriolis data center (IFREMER). The Matlab scripts for the thermal lag correction were taken from the SOCIB Glider toolbox (https://github.com/socib/glider_toolbox). The Matlab seawater toolbox was provided by CSIRO, Australia (http://www.cmar.csiro.au/datacentre/ext_docs/seawater.htm). We thank Glenn Pennycook, MSc, from Liwen Bianji, Edanz Group China (www.liwenbianji.cn/ac), for editing the English text of a draft of this manuscript.

References

Baird M E, Suthers I M, Griffin D A, et al. 2011. The effect of surface flooding on the physical-biogeochemical dynamics of a warm-core eddy off southeast Australia. Deep Sea Research Part II: Topical Studies in Oceanography, 58(5): 592–605, doi: 10.1016/j.dsr2.2010.10.002

Baltes B, Rudnick D, Crowley M, et al. 2014. Toward a U.S. IOOS® Underwater glider network plan: part of a comprehensive subsurface observing system. Technical Report U S IOOS

Böhme L, Send U. 2005. Objective analyses of hydrographic data for referencing profiling float salinities in highly variable environments. Deep Sea Research Part II: Topical Studies in Oceanography, 52(3–4): 651–664, doi: 10.1016/j.dsr2.2004.12.014

Bouffard J, Pascual A, Ruiz S, et al. 2010. Coastal and mesoscale dynamics characterization using altimetry and gliders: a case study in the Balearic sea. Journal of Geophysical Research: Oceans, 115(C10): C10029, doi: 10.1029/2009JC006087

Bouffard J, Renault L, Ruiz S, et al. 2012. Sub-surface small-scale eddy dynamics from multi-sensor observations and modeling. Progress in Oceanography, 106: 62–79, doi: 10.1016/j.pocean.2012.06.007

Dobricic S, Pinardi N, Testor P, et al. 2010. Impact of data assimilation of glider observations in the Ionian Sea (Eastern Mediterranean). Dynamics of Atmospheres and Oceans, 50(1): 78–92, doi: 10.1016/j.dynatmoce.2010.01.001

Dong J L, Domingues R, Goni G, et al. 2017. Impact of assimilating underwater glider data on Hurricane Gonzalo (2014) forecasts. Weather and Forecasting, 32(3): 1143–1159, doi: 10.1175/WAF-D-16-0182.1

Gangopadhyay A, Schmidt A, Agel L, et al. 2013. Multiscale forecasting in the western North Atlantic: Sensitivity of model forecast skill to glider data assimilation. Continental Shelf Research, 63 Suppl: S159–S176

Garau B, Ruiz S, Zhang W G, et al. 2011. Thermal lag correction on Slocum CTD glider data. Journal of Atmospheric and Oceanic Technology, 28(9): 1065–1071, doi: 10.1175/JTECH-D-10-05030.1

Garcia H E, Boyer T, Baranova O K, et al. 2019. World Ocean Atlas 2018: Product Documentation. Silver Spring, Maryland: National Centers for Environmental Information, USA

Liu Z H, Chen X R, Yu J C, et al. 2019. Kuroshio intrusion into the South China Sea with an anticyclonic eddy: Evidence from underwater glider observation. Journal of Oceanology and Limnology, doi: 10.1007/s00343-019-8290-y doi: 10.1007/s00343-019-8290-y

Liu F, Wang Y H, Wu Z L, et al. 2017. Motion analysis and trials of the deep sea hybrid underwater glider Petrel-II. China Ocean Engineering, 31(1): 55–62, doi: 10.1007/s13344-017-0007-4

Liu Y G, Weisberg R H, Lembke C. 2015. Glider salinity correction for unpumped CTD sensors across a sharp thermocline. In: Liu Y G, Kerkering H, Weisberg R H, eds. Coastal Ocean Observing Systems. Amsterdam: Elsevier, 305–325

Liu Z H, Xu J P, Sun C H. 2007. Discussing on detecting and calibration method of Argo conductivity sensor drift errors. Ocean Technology (in Chinese), 26(4): 72–76

Lueck R G, Picklo J J. 1990. Thermal inertia of conductivity cells: observations with a sea-bird cell. Journal of Atmospheric and Oceanic Technology, 7(5): 756–768, doi: 10.1175/1520-0426(1990)007<0756:TIOCCO>2.0.CO;2

Miles T, Seroka G, Kohut J, et al. 2015. Glider observations and modeling of sediment transport in Hurricane Sandy. Journal of Geophysical Research: Oceans, 120(3): 1771–1791, doi: 10.1002/2014JC010474

Morison J, Andersen R, Larson N, et al. 1994. The correction for thermal-lag effects in sea-bird CTD data. Journal of Atmospheric and Oceanic Technology, 11(4): 1151–1164, doi: 10.1175/1520-0426(1994)011<1151:TCFTLE>2.0.CO;2

Oka E, Ando K. 2004. Stability of temperature and conductivity sensors of Argo profiling floats. Journal of Oceanography, 60(2): 253–258, doi: 10.1023/B:JOCE.0000038331.10108.79

Owens W B, Wong A P S. 2009. An improved calibration method for the drift of the conductivity sensor on autonomous CTD profiling floats by θ-S climatology. Deep Sea Research Part I: Oceanographic Research Papers, 56(3): 450–457, doi: 10.1016/j.dsr.2008.09.008

Pan C D, Yaremchuk M, Nechaev D, et al. 2011. Variational assimilation of glider data in Monterey Bay. Journal of Marine Research, 69(2–3): 331–346

Pan C D, Zheng L Y, Weisberg R H, et al. 2014. Comparisons of different ensemble schemes for glider data assimilation on West Florida shelf. Ocean Modelling, 81: 13–24, doi: 10.1016/j.ocemod.2014.06.005

Racape V, Dobler D, Coatanoan C. 2018. Tests RTQC. In: Proceedings of the 19th Meeting of the Argo Data Management Team. San Diego: The 19th Meeting of the Argo Data Managemen Team

Rudnick D L, Davis R E, Eriksen C C, et al. 2004. Underwater gliders for ocean research. Marine Technology Society Journal, 38(2): 73–84, doi: 10.4031/002533204787522703

Ruiz S, Pascual A, Garau B, et al. 2009. Mesoscale dynamics of the Balearic Front, integrating glider, ship and satellite data. Journal of Marine Systems, 78 (Suppl): S3–S16

Shu Y Q, Wang Q, Zu T T. 2018. Progress on shelf and slope circulation in the northern South China Sea. Science China Earth Sciences, 61(5): 560–571, doi: 10.1007/s11430-017-9152-y

Shu Y Q, Xiu P, Xue H J, et al. 2016. Glider-observed anticyclonic eddy in northern South China Sea. Aquatic Ecosystem Health & Management, 19(3): 233–241

Shulman I, Rowley C, Anderson S, et al. 2009. Impact of glider data assimilation on the Monterey Bay model. Deep Sea Research Part II: Topical Studies in Oceanography, 56(3–5): 188–198, doi: 10.1016/j.dsr2.2008.08.003

Stommel H. 1989. The SLOCUM mission. Oceanography, 19(1): 22–25

Tintoré J, Vizoso G, Casas B, et al. 2013. SOCIB: The Balearic Islands Coastal Ocean Observing and Forecasting System Responding

to Science, Technology and Society Needs. Marine Technology Society Journal, 47(1): 101–117, doi: 10.4031/MTSJ.47.1.10

Troupin C, Beltran J P, Heslop E, et al. 2015. A toolbox for glider data processing and management. Methods in Oceanography, 13–14: 13–23, doi: 10.1016/j.mio.2016.01.001

UNESCO. 1981. Tenth report of the joint panel on oceanographic tables and standards. UNESCO technical papers in Marine Sciences, No. 36

U S. Integrated Ocean Observing System. 2016. Manual for quality control of temperature and salinity data observations from gliders Version 1.0. https://cdn.ioos.noaa.gov/media/2017/12/Manual-for-QC-of-Glider-Data_05_09_16.pdf [2017-12-1/2018-8-16]

Wong A P S, Johnson G C, Owens W B. 2003. Delayed-mode calibration of autonomous CTD profiling float salinity data by θ-S climatology. Journal of Atmospheric and Oceanic Technology, 20(2): 308–318, doi: 10.1175/1520-0426(2003)020<0308:DMCOAC>2.0.CO;2

Wong A, Keeley R, Carval T, et al. 2019. Argo quality control manual for CTD and trajectory data. http://dx.doi.org/10.13155/33951 [2018-1-16/2018-8-14]

Yu J C, Zhang A Q, Jin W M, et al. 2011. Development and experiments of the sea-wing underwater glider. China Ocean Engineering, 25(4): 721–736, doi: 10.1007/s13344-011-0058-x